Colloids and Surfaces B: Biointerfaces 107 (2013) 174–179

Contents lists available at SciVerse ScienceDirect

Colloids and Surfaces B: Biointerfaces

journal homepage: www.elsevier.com/locate/colsurfb

Virus inactivation by high frequency ultrasound in combination with visible light

Constantinos V. Chrysikopoulos*, Ioannis D. Manariotis, Vasiliki I. Syngouna

Department of Civil Engineering, Environmental Engineering Laboratory, University of Patras, Patras 26500, Greece

ARTICLE INFO

Article history:
Received 29 September 2012
Received in revised form 16 January 2013
Accepted 16 January 2013
Available online xxx

Keywords:
Disinfection
Ultrasound
Visible light
MS2
ΦX174
Virus inactivation

ABSTRACT

In this study, the effects of high frequency ultrasound (US) and visible light (VL) on virus inactivation were investigated. The bacteriophages ΦX174 and MS2 were used as model viruses. The experiments were performed at room temperature at three different, relatively high US frequencies (i.e., 582, 862, and 1142 kHz) with and without the use of VL, and different initial virus concentrations. The two bacteriophages were diluted in phosphate-buffered saline solution to a titer of 10^3–10^4 pfu/mL. The experimental virus inactivation data were satisfactorily represented by a simple first-order kinetic expression. Virus inactivation was faster at the lower frequencies (582 and 862 kHz). Furthermore, it was observed that MS2 was inactivated faster than ΦX174. The simultaneous use of US and VL was found to be more effective than US alone for MS2 inactivation, indicating the existence of a synergistic effect. However, the use of VL in conjunction with high frequency US hindered the inactivation of ΦX174.

1. Introduction

Waterborne viruses, especially human enteric viruses, are often the cause of numerous outbreaks [1–3]. Although some enteric pathogens may not be a serious health threat to healthy adults, they can present critical health hazard to young children, the elderly, and sick people who often have weak or damaged immune systems [4]. In order to control the spreading of the waterborne diseases, various methods have been routinely employed for the disinfection of water and wastewater. The most commonly used disinfection procedures employ chlorination, ozonation, and ultraviolent irradiation [5]. Worthy to note is that chemical disinfection techniques are not always friendly to the environment. The potential formation of harmful mutagenic and carcinogenic by-products in water and wastewater effluents is a major disadvantage of chemical disinfection [6–8]. However, several more expensive, alternative disinfection technologies are available: gamma irradiation [9], high-energy electron beams [10], streamer corona discharge [11], photocatalysis [12], and ultrasound (US) irradiation [13].

US has been employed for microbial inactivation [13–16] as well as for oxidation of organic contaminants in water [17,18]. US leads to the production of cavitation bubbles, which generate high temperature and pressure at the heart of collapsing bubbles [19,20]. However, microbial inactivation by cavitation is attributed to a combination of simultaneously acting mechanisms: mechanical effects (caused by turbulence generation, microstreaming, liquid circulation currents, and shear stresses) capable of disrupting cell membranes, chemical effects (including generation of active free radicals), and heat effects (i.e. generation of local hot spots) [13,21–23]. Generally, the mechanical effects are more responsible for the microbial disinfection, whereas the chemical and heat effects play only a supporting role [15].

The frequency of US is a very important parameter because it controls the size of the cavitation bubbles [24]. It has been reported in the literature that the mean bubble size increases with increasing acoustic power and decreases with increasing US frequency [25]. In general, high frequency US irradiation has been proven to be effective for the inactivation of *E. coli* [26,27], and microcystins [28]. Sonochemical reaction rate constants are enhanced at high US frequencies (>200 kHz) because the produced free radicals are transported easier away from the cavitation bubbles [29–32]. Furthermore, US in combination with other technologies lead to significantly better microbial inactivation efficiency. Such combinations include US-chlorination [14], US-ultraviolent radiation [33], US-assisted plasma [34], US-titanium dioxide [35]. When US is employed in combination with traditional chemical treatment, the intense pressure gradient improves the penetration of the oxidizing chemicals through the microbial cell membrane [36]. Furthermore, cavitation can facilitate the breakage of microorganism agglomerates [37] and thus increase the efficiency of other chemical disinfectants.

Although the application of US to water treatment is a well-established technology, it is quite difficult to compare the various existing inactivation data sets because of the diverse testing protocols and US systems used. Therefore, more studies are needed before general conclusions can be drawn.

* Corresponding author. Tel.: +30 2610996531; fax: +30 2610996573.
E-mail address: gios@upatras.gr (C.V. Chrysikopoulos).

0927-7765/$ – see front matter © 2013 Elsevier B.V. All rights reserved.
http://dx.doi.org/10.1016/j.colsurfb.2013.01.038

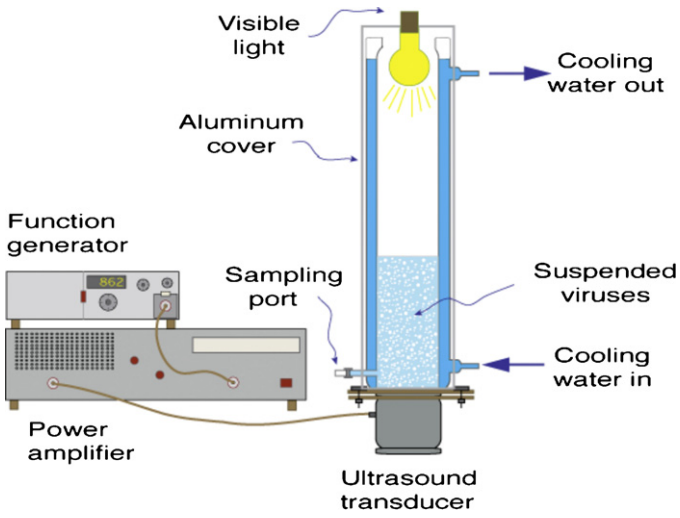

Fig. 1. Illustration of the experimental apparatus.

The aim of this study was to evaluate the effectiveness of high frequency US (582, 862, and 1142 kHz), and US in combination with visible light (US + VL) for the inactivation of model bacteriophages: MS2 and ΦX174, which are often associated with fecal contamination of water supplies. Furthermore, interactions between viruses were estimated in order to avoid false interpretation of the results, due to virus aggregation. To the best of our knowledge the combined effect of high frequency US and VL on virus inactivation has not been explored before.

2. Materials and methods

2.1. Ultrasound reactor

The ultrasonic system employed in this study (Meinhardt Ultraschalltechnik, Leipzig, Germany) consisted of a 75-mm diameter titanium transducer, a function generator, and an amplifier (see Fig. 1). The transducer was mounted at the bottom of a cylindrical 2 L glass reactor with double walls to allow water circulation for cooling. A 550 mL solution of phages suspended in sterile phosphate-buffered saline (PBS: 1.2 mM NaCl, 0.027 mM KCl, and 0.10 mM Na_2HPO_4) at pH = 7 were poured into the glass reactor. A sample of the solution was used to measure and record the initial phage concentration. The solution temperature was measured with a digital thermometer equipped with a thermistor (Oakton Temp 5 Acorn Series, Eutech Instruments Ltd., Singapore), and it was maintained between 27 and 32 °C. The reactor was operated at frequencies ϕ = 582, 862, and 1142 kHz with a power setting of 133 W, or equivalently with a power per unit volume of 0.24 W/mL. Thus, all parameters, except the frequency, ϕ, of the US were maintained constant during the virus inactivation experiments. For each experiment, 2 mL samples were collected at predetermined time intervals over a 120 min time period. The samples were collected from a sampling port located at the bottom of the reactor with a sterile plastic syringe mounted on a stainless steel needle. All samples were analyzed at the end of each experiment.

2.2. Bacteriophage suspensions

The model bacteriophages MS2 and ΦX174 were selected in this study as surrogates for human enteric viruses, which have also been employed in numerous other investigations [38–46]. These bacteriophages are easy to handle because they are not pathogenic, and have similar size and disinfection properties as typical enteric viruses. ΦX174 is an icosahedral, single-stranded DNA phage with 26% nucleic acid content, whose host bacterium is *E. coli* (ATTC 13706-B1); whereas, MS2 is a F-specific, single-stranded RNA phage with 31% nucleic acid content, whose host bacterium is *E. coli* (ATTC 15597-B1). The Φ174 particle diameter ranges from 25 to 27 nm; whereas, MS2 particle diameter ranges from 24 to 26 nm. ΦX174 has hydrophilic protein coat; whereas, MS2 has hydrophobic protein coat [47]. The bacteriophages ΦX174 and MS2, were suspended and diluted in PBS solution at pH = 7 to concentrations in the range of 10^3–10^4 pfu/mL. Both bacteriophages were assayed by the double-layer overlay method [48], where 0.1 mL solution containing the appropriate host bacterium and 0.1 mL of a diluted virus sample solution collected, were mixed in a centrifuge tube. The mixture was combined with molten soft-agar medium (4.5 mL), maintained at 45 °C in a tube, and poured onto a petri dish containing solid agar medium. The plates were solidified for 10 min and incubated overnight at 37 °C. Viable virus concentrations were determined by counting the number of plaques in each host lawn and reported as plaque-forming units per milliliter (pfu/mL). Only dilutions that resulted in 20–300 plaques per plate were accepted for quantification. All virus concentrations reported in this study represent the average of three replicate plates (n = 3). However, this technique could lead to concentration underestimation because discrete viruses and virus aggregates may not be differentiated. Note that either a solo virus or a virus aggregate produces just one plaque-forming unit. However, virus aggregation is minimized at pH = 7 [49]. Furthermore, to reduce the inherit disadvantage of the analytical technique employed, the samples were stirred and three replicate plates were used for each concentration measurement.

3. Theoretical considerations

3.1. Virus aggregation

The effect of virus aggregation as influenced by solution chemistry can be a complicated issue, and is interpreted in this study by estimation of the virus interfacial potential energy with the Derjaguin, Landau, Verwey and Overbeek (DLVO) theory [50,51]. The classical DLVO theory indicates that the total interaction energy between two surfaces is determined by the van der Waals, Φ_{vdW}; double layer, Φ_{dl}; and Born, Φ_{Born}, potential energies [52]:

$$\Phi_{DLVO}(h) = \Phi_{vdW}(h) + \Phi_{dl}(h) + \Phi_{Born}(h) \quad (1)$$

where h is the separation distance between the approaching surfaces. For two approaching spherical surfaces the analytical expressions for Φ_{vdW} and Φ_{Born} have been determined by Feke et al. [53], and for Φ_{dl} by Hogg et al. [54]. However, the classical DLVO theory has not been always successful to describe particle interactions [55]. The discrepancy between experimental data and theory is attributed to additional energies such as the hydration pressure, hydrogen bonding forces, hydrophobic effects, disjoining pressure, structural forces, osmotic forces, elastic forces and Lewis acid–base forces [56–60]. Incorporation of additional energies of interaction into the classic DLVO model leads to the extended-DLVO (XDLVO) theory. In this study, according to the XDLVO theory, the total interaction energy between two approaching surfaces is considered as the sum of the classical DLVO, Φ_{DLVO}, and Lewis acid–base, Φ_{AB}, interaction energies:

$$\Phi_{XDLVO}(h) = \Phi_{DLVO}(h) + \Phi_{AB}(h) \quad (2)$$

The appropriate analytical expression describing Φ_{AB} for the case of two approaching spherical surfaces has been reported by van Oss [57].

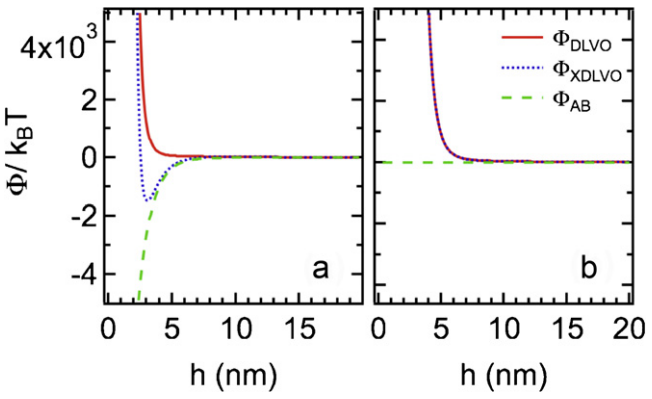

Fig. 2. Predicted sphere–sphere Φ_{DLVO} (solid curves), Φ_{AB} (dotted curves), and Φ_{XDLVO} (dashed curves) interaction energy profiles for (a) MS2-MS2, and (b) ΦX174–ΦX174 as a function of separation distance, for the experimental conditions.

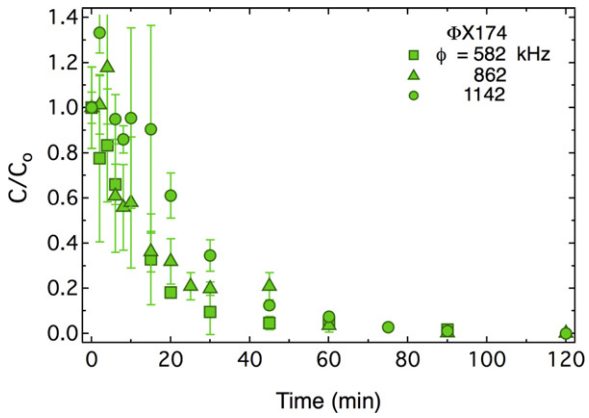

Fig. 3. Normalized experimental data with associated error bars (±SD, $n = 3$) for ΦX174 inactivation by US at three different acoustic frequencies. Error bars not shown are smaller than the size of the symbol.

3.2. Inactivation kinetics

The experimental data from numerous inactivation studies have been successfully described by the following pseudo-first-order expression with a time-dependent rate coefficient [61–64]:

$$\frac{dC(t)}{dt} = -\lambda(t)C(t) \quad (3)$$

where C is the concentration of suspended viruses in the liquid phase, t is time, and λ is the time-dependent inactivation rate coefficient of suspended viruses described by the following expression [61]:

$$\lambda(t) = \lambda_0 e^{-\alpha t} \quad (4)$$

where λ_0 is the initial inactivation rate coefficient, and α is the resistivity coefficient. Assuming that $C(0) = C_0$, where C_0 is the initial virus concentration, the solution to Eq. (3) is:

$$\ln\left[\frac{C(t)}{C_0}\right] = -\frac{\lambda_0}{\alpha}\left[e^{-\alpha t} - 1\right] \quad (5)$$

For the special case where $\lambda(t) = \lambda$ the solution to Eq. (3) is:

$$\ln\left[\frac{C(t)}{C_0}\right] = -\lambda t \quad (6)$$

The unknown inactivation parameter values λ_0 and α were obtained by fitting Eq. (5) to the experimental log-normalized-concentration data using non-linear least squares algorithms, whereas the unknown parameter λ was estimated by linear regression fit of Eq. (6) to the log-normalized experimental data.

4. Results and discussion

In order to evaluate the possibility of virus aggregation, the Φ_{DLVO}, Φ_{AB}, and Φ_{XDLVO} interaction energy profiles as applied to identical virus–virus interactions were constructed following previously published procedures and parameter values [43]. The predicted energy profiles under the experimental conditions (PBS solution: pH = 7, ionic strength $I_s = 2$ mM) were constructed for the case of sphere–sphere approximation (assuming that both bacteriophages are spherical), and are shown in Fig. 2. Clearly, the classical DLVO theory suggested that MS2 and ΦX174 suspensions were very stable, and no aggregation between like particles was expected to occur under the experimental conditions. The repulsive potential was high and the total potential remained positive for long separation distances. However, the XDLVO theory predicted a primary minimum for the MS2–MS2 case (see dotted curve in Fig. 2a), and suggested that Φ_{AB} hydrophobic interactions between MS2 particles could lead to initial aggregation. Therefore, Lewis acid–base interactions play an important role in the total interaction energy for the MS2–MS2 case. MS2 particles also have been shown in previous studies to aggregate in ddH_2O [43]. Significant coagulation should be expected at pH values near the pH of the isoelectric point, pH_{iep}, which represents the pH where the surface charge of a suspended particle is neutralized. In ddH_2O, the pH_{iep} of MS2 and ΦX174 were reported to be 4.1 and 4.4, respectively [43]. However, it should be noted that the pH_{iep} of bacteriophages varies slightly with I_s fluctuations [65].

Fig. 3 presents the results from the ΦX174 inactivation experiments with US for three different acoustic frequencies ($\phi = 582$, 862, and 1142 kHz). The concentrations for each experiment were normalized with respect to the initial ΦX174 concentration, which for the three inactivation experiments were 1176, 586 and 608 pfu/mL for the frequencies 582, 862 and 1142 kHz, respectively. Clearly, faster inactivation of ΦX174 was observed at the lower acoustic frequencies.

Fig. 4 presents the results from the MS2 inactivation experiments with US for the two lower acoustic frequencies ($\phi = 582$, and 862 kHz). Three different initial concentrations were used for $\phi = 582$ kHz in order to investigate the effect of initial concentration on inactivation. The initial MS2 concentrations for the four inactivation experiments were 11,175, 14,025, 10,783, and 17,700 pfu/mL for the frequencies 582(a), 582(b), 582(c), and 862 kHz, respectively. The experimental data suggested that virus inactivation was affected by the initial virus concentration. Worthy to note is that

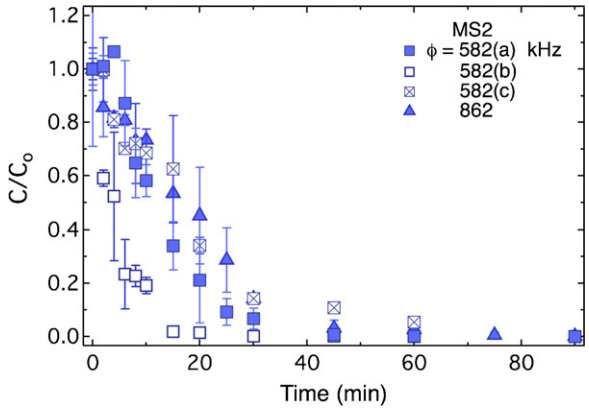

Fig. 4. Normalized experimental data with associated error bars (±SD, $n = 3$) for MS2 inactivation by US at two different acoustic frequencies. Error bars not shown are smaller than the size of the symbol.

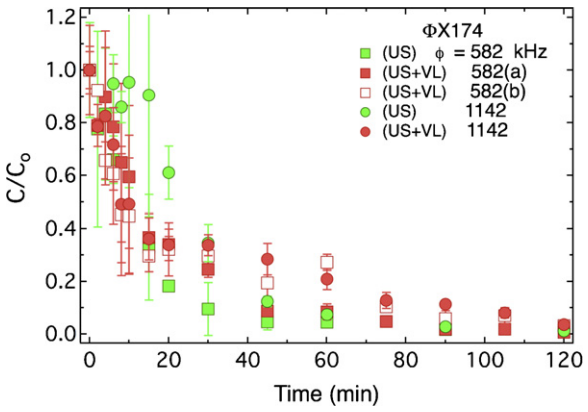

Fig. 5. Normalized experimental data with associated error bars (±SD, $n = 3$) for ΦX174 inactivation by US and combined US + VL at two different acoustic frequencies. Error bars not shown are smaller than the size of the symbol.

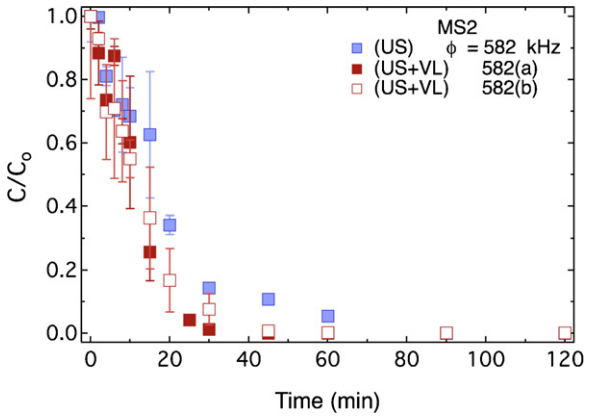

Fig. 6. Normalized experimental data with associated error bars (±SD, $n = 3$) for MS2 inactivation by US and combined US + VL at 582 kHz. Error bars not shown are smaller than the size of the symbol.

MS2 inactivation rates increased with increasing initial virus concentration.

Fig. 5 presents the experimental results from ΦX174 inactivation experiments with US alone and with combined US + VL for the low and high acoustic frequencies ($\phi = 582$ and 1142 kHz). Two different initial concentrations were used for the inactivation experiments with combined US + VL for $\phi = 582$ kHz. The initial ΦX174 concentrations for the inactivation experiments with combined US + VL were 6388, 3690, and 5125 pfu/mL for the frequencies 582(a), 582(b), and 1142 kHz, respectively. Whereas, the initial ΦX174 concentrations for the inactivation experiments with US were 1176 and 608 pfu/mL for $\phi = 582$ and 1142 kHz, respectively. Clearly, ΦX174 inactivation with US + VL hinders the inactivation of ΦX174 compared to the inactivation experiments with high frequency US alone. Furthermore, the experimental data suggested that ΦX174 inactivation rates increased with increasing initial virus concentration. This observation is in agreement with the MS2 inactivation results obtained for the inactivation experiments with high frequency US alone (see Fig. 4).

In a recent study of ΦX174 and MS2 inactivation in the presence of quartz sand under static and dynamic batch conditions, contrary to the results of this study, it was observed that the inactivation rates decreased with increasing initial virus concentrations [60]. Possible explanations for this discrepancy could be either that the distractive cavitation effects are expected to be more pronounced as the virus concentrations increase because more cavitation bubbles are in the neighborhood of suspended bacteriophages, or when virus aggregates are present because are expected to form easier at higher concentrations. The second explanation could be valid only for MS2 because for the case of ΦX174 no aggregation is expected under the experimental conditions (see Fig. 2b). Worthy to note is that virus aggregation in the absence of US is known to reduce significantly inactivation rates [66]. However, aggregation may not protect viruses from the high temperature and pressure generated by the cavitation bubbles when US is applied. Certainly, more experiments are needed in order to fully understand the mechanisms that lead to the observed inactivation behavior of ΦX174 and MS2.

Fig. 6 presents the experimental results from MS2 inactivation with US alone and with combined US + VL for the low acoustic frequency ($\phi = 582$ kHz). Two different initial concentrations were used for the inactivation experiments with US + VL. The initial MS2 concentrations for the inactivation experiments with combined US + VL were 11,133, and 7500 pfu/mL for the frequencies 582(a), and 582(b), respectively. Whereas, the initial MS2 concentration for the inactivation experiment with US was 10,783 pfu/mL. Clearly, MS2 inactivation with US + VL enhances the inactivation of MS2 compared to the MS2 inactivation with high frequency US alone. Worthy to note is that this observation is exactly opposite than that observed for ΦX174 inactivation. Therefore, it appears that VL acts synergistically with US on MS2 inactivation, but ΦX174 is more resistant to the combined effects of inactivation with US + VL. Furthermore, the experimental data suggested that MS2 inactivation rates were increased with increasing initial virus concentration. This observation was in agreement with the MS2 inactivation results with high frequency US alone (see Fig. 4), and ΦX174 inactivation results with US + VL (see Fig. 5). MS2 inactivation enhancement by VL irradiation was also observed by other investigators [67]. A possible explanation for the observed synergistic effect is that MS2 absorbs the incident photon energy [68], which leads to photo-induced reactions in conjunction with the collapsing cavitation bubbles produced by high frequency US [19,20].

Fig. 7 presents selected ΦX174 and MS2 inactivation experimental data together with the fitted models for both constant and time-dependent inactivation rate coefficients. Clearly, both inactivation models simulate the experimental data quite satisfactorily. Therefore, the simple first-order inactivation model with constant inactivation rate coefficients is recommended. The fitted inactivation rate coefficients for all experiments conducted in this study are listed in Table 1. Similar inactivation rates with those obtained here have been reported for MS2 by other researchers that employed sunlight, photocatalysis, and various chemicals. Mattle et al. [69] reported that the inactivation rate of MS2 ranged from $\lambda = 0.05$ to 0.17 1/min. Hu et al. [70] observed that MS2 inactivation with 2.8 mg/L potassium ferrate (VI) at pH = 8.0, and $C_0 = 4 \times 10^9$ pfu/mL underwent with a rate of $\lambda = 0.29$ 1/min. Simulated sunlight irradiation of MS2 resulted in inactivation rates ranging from $\lambda = 0.00008$

Table 1
Fitted values ± one standard deviation (±SD) of the inactivation rate coefficients.

Conditions	C_0 (pfu/mL)	ϕ (kHz)	λ (1/min)
ΦX174			
US	1176	582	0.055 ± 0.002
US	586	862	0.053 ± 0.004
US	608	1142	0.039 ± 0.002
US + VL	6388	582(a)	0.042 ± 0.001
US + VL	3690	582(b)	0.029 ± 0.002
US + VL	5125	1142	0.027 ± 0.002
MS2			
US	11,175	582(a)	0.103 ± 0.005
US	14,025	582(b)	0.193 ± 0.013
US	10,783	582(c)	0.050 ± 0.002
US	17,700	862	0.067 ± 0.002
US + VL	11,133	582(a)	0.123 ± 0.011
US + VL	7500	582(b)	0.073 ± 0.005

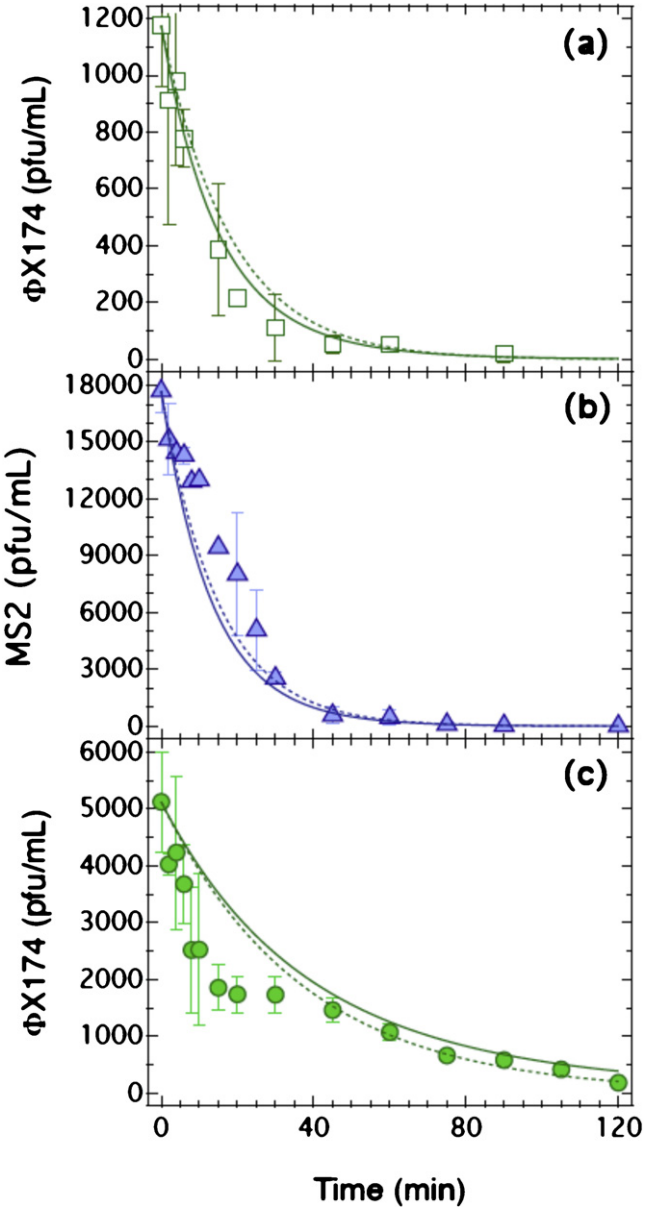

Fig. 7. Virus concentration data (symbols) with associated error bars (±SD, $n = 3$) and fitted models (curves) for (a) ΦX174 inactivation by US at $\phi = 582$ kHz, (b) MS2 inactivation by US at $\phi = 862$ kHz, and (c) ΦX174 inactivation by combined US + VL at 1142 kHz. The dotted and solid curves correspond to constant and time-dependent rate inactivation, respectively. Error bars not shown are smaller than the size of the symbol.

to 0.0025 1/min [71] or $\lambda \leq 0.063$ 1/min in the absence of natural organic matter [72]. Note that the virus inactivation rates due to US or US + VL reported in Table 1 are at least three orders of magnitude larger than ΦX174 and MS2 inactivation rates determined under laboratory (static and dynamic) and field conditions reported by other investigators [63,64,73].

Fig. 8 presents graphically the variability of the fitted inactivation rate coefficient as a function of initial virus concentration and acoustic frequency for the inactivation experiments with US and US + VL. A clear trend of increasing inactivation with increasing initial virus concentration is shown. Furthermore, the fitted inactivation rate coefficients clearly suggest that MS2 inactivation is faster than that of ΦX174. This result is in agreement with other studies published in the recent literature [64,74,75].

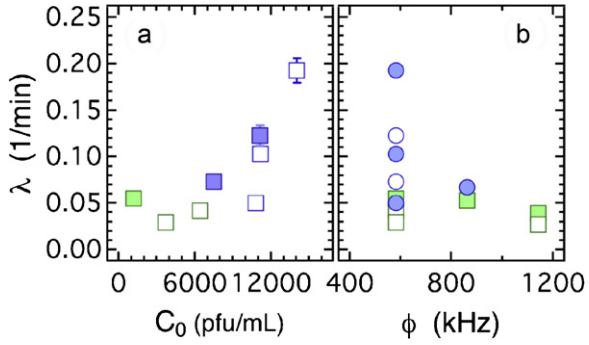

Fig. 8. Fitted inactivation rate coefficients and associated error bars (±SD) for ΦX174 (squares) and MS2 (circles) as a function of (a) initial virus concentration at $\phi = 582$ kHz, and (b) acoustic frequency. The solid symbols represent inactivation by US, and the open symbols inactivation by US + VL. Error bars not shown are smaller than the size of the symbol.

5. Summary and conclusions

High frequency US (582, 862, and 1142 kHz), and US in combination with VL were employed in order to experimentally investigate the inactivation of MS2 and ΦX174. Various experiments were conducted at room temperature and the virus inactivation data were satisfactorily represented by a simple first-order kinetic expression. Possible interactions between viruses were theoretically estimated so that the extent of virus aggregation under the experimental conditions could be evaluated. The experimental data suggested that, for both viruses, the inactivation due to US was faster at the lower frequency examined, and that MS2 inactivation was relatively faster than ΦX174 inactivation. Furthermore, for the case of MS2 it was shown that US + VL was more effective than US alone. For the case of ΦX174, US and VL did not provide any synergistic effects, on the contrary, the inactivation of ΦX174 was hindered. Therefore, the combined use of US and VL should be employed only on specific cases.

Acknowledgments

This research has been co-financed by the European Union (European Social Fund-ESF) and Greek National Funds through the Operational program "Education and Lifelong Learning" under the action Aristeia I (Code No. 1185). This work is a collaboration between members of the BioMet Network, University of Patras.

References

[1] J.E. Scandura, M.D. Sobsey, Water Sci. Technol. 35 (11–12) (1997) 141–146.
[2] R. Anders, C.V. Chrysikopoulos, Water Resour. Res. 41 (10) (2005) W10415, http://dx.doi.org/10.1029/2004WR003419.
[3] G.F. Craun, M.F. Craun, R.L. Calderon, M.J. Beach, J. Water Health 4 (2006) 19–30.
[4] J. Theron, T.E. Cloete, Crit. Rev. Microbiol. 28 (1) (2002) 1–26.
[5] G.C. White, Handbook of Chlorination and Alternative Disinfectants, Van Nostrand Reinhold Publishing, New York, 1992.
[6] R.A. Minear, G.L. Amy (Eds.), Disinfection By-products in Water Treatment, CRC Press Inc., Boca Raton, 1996.
[7] A. Adin, J. Katzhendler, D. Alkaslassy, Ch. Rav-Acha, Water Res. 25 (7) (1991) 797–805.
[8] W.A. Mitch, D.L. Sedlak, Environ. Sci. Technol. 36 (4) (2002) 588–595.
[9] J.E. Thompson, E.R. Blatchley, J. Environ. Eng. 126 (8) (2000) 761–768.
[10] S. Farooq, C.N. Kurucz, T.D. Waite, W.J. Cooper, S.R. Mane, J.H. Greenfield, Water Sci. Technol. 26 (1992) 1265–1274.
[11] C. Lee, J. Kim, J. Yoon, Chemosphere 82 (8) (2011) 1135–1140.
[12] S. Malato, P. Fernandez-Ibanez, M.I. Maldonado, J. Blanco, W. Gernjak, Catal. Today 147 (1) (2009) 1–59.
[13] P. Piyasena, Int. J. Food Microbiol. 87 (3) (2003) 207–216.
[14] S.S. Phull, A.P. Newman, J.P. Lorimer, B. Pollet, T.J. Mason, Ultrason. Sonochem. 4 (1997) 157–164.
[15] T.J. Mason, E. Joyce, S.S. Phull, J.P. Lorimer, Ultrason. Sonochem. 10 (6) (2003) 319–323.
[16] P.R. Gogate, A.M. Kabadi, Biochem. Eng. J. 44 (2009) 60–72.

[17] N.N. Mahamuni, Y.G. Adewuyi, Ultrason. Sonochem. 17 (6) (2010) 990–1003.
[18] I.D. Manariotis, H.K. Karapanagioti, C.V. Chrysikopoulos, Water Res. 45 (2011) 2587–2594.
[19] K.S. Suslick, Sci. Am. 260 (2) (1989) 80–86.
[20] D.J. Flannigan, K.S. Suslick, Nature 434 (2005) 52–55.
[21] M.S. Doulah, Biotechnol. Bioeng. 19 (5) (1977) 649–660.
[22] G. Scherba, R.M. Weigel, W.D. O'Brien Jr., Appl. Environ. Microbiol. 57 (7) (1991) 2079–2084.
[23] P.R. Gogate, J. Environ. Manage. 85 (2007) 801–815.
[24] K.S. Suslick, Sonochemistry, Science 247 (4949) (1990) 1439–1445.
[25] A. Brotchie, F. Grieser, M. Ashokkumar, Phys. Rev. Lett. 102 (2009) 084302.
[26] R.V. Peterson, W.G. Pitt, Colloids Surf. B: Biointerfaces 17 (2000) 219–227.
[27] I. Hua, J.E. Thompson, Water Res. 34 (15) (2000) 3888–3893.
[28] B. Ma, Y. Chen, H. Hao, M. Wu, B. Wang, H. Lv, G. Zhang, Colloids Surf. B: Biointerfaces 41 (2005) 197–201.
[29] I. Hua, M.R. Hoffmann, Environ. Sci. Technol. 31 (1997) 2237–2243.
[30] C. Petrier, A. Jeunet, J.-L. Luche, G. Reverdy, J. Am. Chem. Soc. 114 (1992) 3148–3150.
[31] C. Petrier, M.F. Lamy, A. Fancony, A. Benahcene, B. David, V. Renaudin, N. Gondrexon, J. Phys. Chem. 98 (1994) 10514–10520.
[32] C. Petrier, B. David, S. Laguian, Chemosphere 32 (1996) 1709–1718.
[33] V. Naddeo, V. Belgiorno, M. Landi, T. Zarra, R.M. Napoli, Desalination 249 (2) (2009) 762–767.
[34] C.W. Chen, H.M. Lee, S.H. Chen, H.L. Chen, M.B. Chang, Environ. Sci. Technol. 43 (12) (2009) 4493–4497.
[35] M. Dadjour, C. Ogino, S. Matsumura, N. Shimizu, Biochem. Eng. J. 25 (3) (2005) 243–248.
[36] E.V. Rokhina, P. Lens, J. Virkutyte, Trends Biotechnol. 27 (5) (2009) 298–306.
[37] Y. Chisti, M. Moo-Young, Enzyme Microb. Technol. 8 (1986) 194–204.
[38] J.F. Schijven, W. Hoogenboezem, S.M. Hassanizadeh, J.H. Peters, Water Resour. Res. 35 (1999) 1101–1111.
[39] A.A. Keller, S. Sirivithayapakorn, C.V. Chrysikopoulos, Water Resour. Res. 40 (2004) W08304, http://dx.doi.org/10.1029/2003WR002676.
[40] P.W.J.J. van der Wielen, W.J.M.K. Senden, G. Medema, Environ. Sci. Technol. 42 (2008) 4589–4594.
[41] R. Anders, C.V. Chrysikopoulos, Transport Porous Med. 76 (2009) 121–138.
[42] G.E. Walshe, L. Pang, M. Flury, M.E. Close, M. Flintoft, Water Res. 44 (2010) 1255–1269.
[43] C.V. Chrysikopoulos, V.I. Syngouna, Colloids Surf. B: Biointerfaces 92 (2012) 74–83, http://dx.doi.org/10.1016/j.colsurfb.2011.11.028.
[44] Y. Azimi, D.G. Allen, R.R. Farnood, Water Res. 46 (2012) 3827–3836.
[45] B.M. Pecson, L. Decrey, T. Kohn, Water Res. 46 (2012) 1763–1770.
[46] V.I. Syngouna, C.V. Chrysikopoulos, Colloids Surf. A: Physicochem. Eng. Aspects 416 (2013) 56–65.
[47] P.A. Shields, Factors Influencing Virus Adsorption to Solids. Ph.D. Dissertation, University of Florida, Gainesville, FL, 1986.
[48] M.H. Adams, Bacteriophages, Interscience, New York, N.Y., 1959, pp. 450–454.
[49] R. Floyd, D.G. Sharp, Appl. Environ. Microbiol. 33 (1977) 159–167.
[50] B.V. Derjaguin, L.D. Landau, Acta Physicochim. U.S.S.R 14 (1941) 733–762.
[51] E.J. Verwey, J.T.G. Overbeek, Theory of the Stability of Lyophobic Colloids, Elsevier, Amsterdam, 1948.
[52] J.P. Loveland, J.N. Ryan, G.L. Amy, R.W. Harvey, Colloids Surf. A: Physicochem. Eng. Aspects 107 (1996) 205–221.
[53] D.L. Feke, N.D. Prabhu, J.A. Mann Jr., J.A. Mann III, J. Phys. Chem. 88 (1984) 5735–5739.
[54] R. Hogg, T.W. Healy, D.W. Fuerstenau, Trans. Faraday Soc. 62 (1966) 1638–1651.
[55] C.J. van Oss, Colloids Surf. A: Physicochem. Eng. Aspects 78 (1993) 1–49.
[56] J.N. Israelachvili, Intermolecular and Surface Forces, second ed., Academic Press, London, 1992.
[57] C.J. van Oss, Interfacial Forces in Aqueous Media, Marcel Dekker, New York, 1994.
[58] S.W. Swanton, Adv. Colloid Interface Sci. 54 (1995) 129–208.
[59] J. Bergendahl, D. Grasso, AIChE J. 45 (3) (1999) 475–484.
[60] J.E. Song, T. Phenrat, S. Marinakos, Y. Xiao, J. Liu, M.R. Wiesner, R.D. Tilton, G.V. Lowry, Environ. Sci. Technol. 45 (14) (2011) 5988–5995.
[61] Y. Sim, C.V. Chrysikopoulos, Water Resour. Res. 32 (1996) 2607–2611.
[62] C.V. Chrysikopoulos, E.T. Vogler, Stoch. Environ. Res. Risk Assess 18 (2004) 67–78.
[63] R. Anders, C.V. Chrysikopoulos, Environ. Sci. Technol. 40 (2006) 3237–3242.
[64] C.V. Chrysikopoulos, A.F. Aravantinou, J. Hazard. Mater. 233–234 (2012) 148–157.
[65] B.L. Yuan, M. Pham, T.H. Nguyen, Environ. Sci. Technol. 42 (20) (2008) 7628–7633.
[66] M.J. Mattle, B. Crouzy, M. Brennecke, K.R. Wigginton, P. Perona, T. Kohn, Environ. Sci. Technol. 45 (2011) 7710–7717.
[67] J.Y. Kim, C. Lee, M. Cho, J. Yoon, Water Res. 42 (1–2) (2008) 356–362.
[68] T.B. Richardson, C.D. Porter, Virology 341 (2005) 321–329.
[69] M.J. Mattle, B. Crouzy, M. Brennecke, K.R. Wiggington, P. Perona, T. Kohn, Environ. Sci. Technol. 45 (18) (2011) 7710–7717.
[70] L. Hu, M.A. Page, T. Sigstam, T. Kohn, B.J. Marinas, T.J. Strathmann, Environ. Sci. Technol. 46 (21) (2012) 12079–12087.
[71] M.B. Fisher, D.C. Love, R. Schuech, K.R. Nelson, Environ. Sci. Technol. 45 (21) (2011) 9249–9255.
[72] O.C. Romero, A.P. Straub, T. Kohn, T.H. Nguyen, Environ. Sci. Technol. 45 (24) (2011) 10385–10393.
[73] J.F. Schijven, S.M. Hassanizadeh, Removal of viruses by soil passage: overview of modeling, processes and parameters, Crit. Rev. Environ. Sci. Technol. 30 (2000) 49–127.
[74] V.I. Syngouna, C.V. Chrysikopoulos, Environ. Sci. Technol. 44 (2010) 4539–4544.
[75] V.I. Syngouna, C.V. Chrysikopoulos, J. Contam. Hydrol. 126 (2011) 301–314.